JOURNAL OF COMPUTATIONAL PHYSICS **126,** 40–51 (1996)
ARTICLE NO. 0118

Wavelet and Finite Element Solutions for the Neumann Problem Using Fictitious Domains

ROLAND GLOWINSKI,* T. W. PAN,* RAYMOND O. WELLS JR.,† AND XIAODONG ZHOU†

Department of Mathematics, University of Houston, Texas 77004; †Department of Mathematics, Rice University, P.O. Box 1892, Houston, Texas 77251

Received February 15, 1995

This paper presents a new fictitious domain formulation for the solution of a strongly elliptic boundary value problem with Neumann boundary conditions for a bounded domain in a finite-dimensional Euclidean space with a smooth (possibly only Lipschitz) boundary. This extends the domain to a larger rectangular domain with periodic boundary conditions for which fast solvers are available. The extended solution converges on the original domain in the appropriate function spaces as the penalty parameter approaches zero. Both wavelet-Galerkin and finite elements numerical approximation schemes are developed using this methodology. The convergence rates of both schemes are comparable, and the use of finite elements requires a parameterization of the boundary, while the wavelet-Galerkin method admits an implicit description of the boundary in terms of a wavelet representation of the boundary measure defined as the distributional gradient of the characteristic function of the interior. The accuracy of both methods is investigated and compared, both theoretically and for numerical test cases. The conclusion is that the methods are comparable, and that the wavelet method allows the use of more general boundaries which are not explicitly parametrized, which would be of greater advantage in higher dimensions (the numerical tests are carried out in two dimensions).

CONTENTS

1. INTRODUCTION

The Neumann problem in two dimensions is a classical test case for any elliptic solver. In this paper we bring together several new ideas and compare them with more classical techniques. There are several fundamental ingredients coming together here:

- The boundary value problem is formulated for an open domain with a rectifiable boundary of any shape.
- The given domain is embedded in a larger and simpler domain (usually rectilinear in shape).
- The elliptic boundary-value problem in the original domain is reformulated in a weak form as an integral equation in the larger domain, and this involves introducing a regularization parameter ε (the so-called penality parameter). Solutions depending on ε converge to solutions of the original equation as ε converges to zero.
- Both wavelet and finite-element Galerkin type methods are used for numerical approximations in the larger domain for fixed and small values of ε.
- Due to the rectinlinear nature of the larger domain, fast periodic solvers can be implemented in the larger domain.

Earlier work on fictitious domains is discussed in the sections below. In Section 2 we discuss the variational formulation of the Neumann problem which will set the framework for the rest of the paper. In Section 3 we formulate the fictitious domain extension of our boundary-value problem to a larger simpler domain and prove a convergence theorem which asserts that as the penalty parameter ε tends to zero the regularized solution of the problem u_ε converges to a solution of the boundary-value problem. In Section 4, we consider the finite element approximation of the regularized Neumann problem and the error estimate of the finite element solution.

2. THE NEUMANN PROBLEM FOR ELLIPTIC OPERATORS: VARIATIONAL FORMULATIONS

2.1. *Generalities*

Let ω be a bounded open connected set (i.e., a domain) of $\mathbf{R}^d$ ($d \geq 1$), and let us denote by γ the boundary $\partial\omega$ of

0021-9991/96 $18.00

ω. We assume that the domain ω is a $C^{k,\alpha}$ domain, $k \in \mathbf{Z}$, $k \geq 0$, $0 \leq \alpha \leq 1$. This means that $\partial\omega$ is defined by a function $F \in C^{k,\alpha}(\mathbf{R}^d)$; i.e., F has continuous derivatives of order k and the partial derivatives of F of order k are Hölder continuous of order α. Special cases of this that we will use in this paper are that ω is a $C^{0,1}$ domain (Lipschitz domain), in which any $g \in H^1(\omega)$ extends to a function $\tilde{g} \in H^1(\Omega)$, and ω is a $C^{1,1}$ domain, in which case any $g \in H^2(\omega)$ extends to a function $\tilde{g} \in H^2(\Omega)$. Both of these types of extensions will play an important role in this paper.

Various applications from physics, mechanics, and engineering lead one to consider the solution of the following problem:

$$-\nabla \cdot \mathbf{A}\nabla u + a_0 u = f \quad \text{in } \omega, \tag{2.1}$$

$$\mathbf{A}\nabla u \cdot \mathbf{n} = g \quad \text{on } \partial\omega. \tag{2.2}$$

In (2.1), (2.2) we use the standard notation

$$\nabla = \left\{\frac{\partial}{\partial x_i}\right\}_{i=1}^{d},$$

where $x = \{x_i\}_{i=1}^d$ is the generic point in $\mathbf{R}^d$. Moreover, we set

$$\nabla \cdot \mathbf{V} = \sum_{i=1}^{d} \frac{\partial V_i}{\partial x_i}, \quad \mathbf{a} \cdot \mathbf{b} = \sum_{i=1}^{d} a_i b_i,$$

where $\mathbf{V} = \{V_i\}_{i=1}^d$ is a vector-valued function, $\mathbf{a} = \{a_i\}_{i=1}^d$, $\mathbf{b} = \{b_i\}_{i=1}^d$ are vectors in $\mathbf{R}^d$ (distinguishing between vectors and points in $\mathbf{R}^d$ in this context for clarity), and where $\mathbf{n}$ is the unit vector of the outward normal to $\partial\omega$ at a generic point. In addition we assume positivity properties of the coefficients to make it an elliptic problem. Namely, we assume that

$$a_0 \in L^\infty(\omega),\ a_0(x) \geq 0, \quad \text{a.e. on } \omega,\ a_0 \neq 0, \tag{2.3}$$

and, moreover, that $\mathbf{A}$ is a $d \times d$ matrix whose entries a_{ij} belong to $L^\infty(\omega)$ and which satisfies the ellipticity property

$$\mathbf{A}(x)\xi \cdot \xi \geq \alpha|\xi|^2, \quad \text{a.e. on } \omega,\ \forall \xi \in \mathbf{R}^d, \tag{2.4}$$

where, in (2.4), α is a *positive* constant and $|\xi|^2 = \xi \cdot \xi$. Finally we assume that the input data f and g satisfy regularity conditions of the form:

$$f \in L^2(\omega),\ g \in H^{-1/2}(\partial\omega). \tag{2.5}$$

Remark. We can take for f mathematical objects which are much less regular than a $L^2(\omega)$-function. For example, f can be a measure supported by a $(d-1)$-manifold contained in ω. In fact, the various methods to be described in the following parts of this article will apply to these situations.

The main goal of this article is to discuss a solution methodology for problem (2.1), (2.2) based on the so-called fictitious (or embedding) domain concept; fictitious domain formulations (to be described in Section 3) heavily rely on the variational formulations for the Neumann problem (2.1), (2.2) to be discussed in the next section.

2.2. *Variational Formulation of the Neumann Problem*

Following, e.g., [7], we derive a *variational formulation* of problem (2.1) by multiplying both sides of Eq. (2.1) by $v \in H^1(\omega)$ and then applying the *divergence theorem.* We obtain then (with $dx = dx_1 \cdots dx_d$)

$$\begin{aligned}\int_\omega (-\nabla \cdot \mathbf{A}\nabla u v + a_0 u v)\, dx &= \int_\omega (\mathbf{A}\nabla u \cdot \nabla u + a_0 u v)\, dx - \int_{\partial\omega} \mathbf{A}\nabla u \cdot \mathbf{n} v\, d\gamma \\ &= \int_\omega f v\, dx,\end{aligned}$$

where $d\gamma$ is the induced Lebesgue measure on $\partial\omega$. Combining this with (2.2) implies that u satisfies (at least formally)

$$\int_\omega (\mathbf{A}\nabla u \cdot \nabla v + a_0 u v)\, dx = \int_\omega f v\, dx + \langle g, v\rangle \quad \forall v \in H^1(\omega), \tag{2.6}$$

where $\langle \cdot, \cdot \rangle$ denotes the duality pairing between $H^{-1/2}(\partial\omega)$ and $H^{1/2}(\partial\omega)$. Relation (2.6) is at the basis of a classical *variational formulation* of the Neumann problem, since it can be shown that if a function $u \in H^1(\omega)$ satisfies (2.6) then it is also a solution of problem (2.1), (2.2), the derivatives in (2.1) being taken in the distribution sense. The variational formulation of (2.1), (2.2) derived from (2.6) becomes

$$\begin{aligned}&\textit{Find } u \in H^1(\omega) \textit{ such that } \forall v \in H^1(\omega) \textit{ we have} \\ &\int_\omega (\mathbf{A}\nabla u \cdot \nabla v + a_0 u v)\, dx = \int_\omega f v\, dx + \langle g, v\rangle.\end{aligned} \tag{2.7}$$

It is shown in, e.g., [7], that problem (2.7) has (as a consequence of the *Lax–Milgram lemma*) a *unique* solution if (2.3)–(2.5) hold.

Formulation (2.7) is at the basis of powerful *Galerkin-type* solution methods such as *finite elements* (see, e.g., [13, 7, 2, 1]). In this article, we shall combine it with fictitious domain techniques in order to derive solution methods well suited to wavelet and finite element approximations taking advantage of Cartesian meshes.

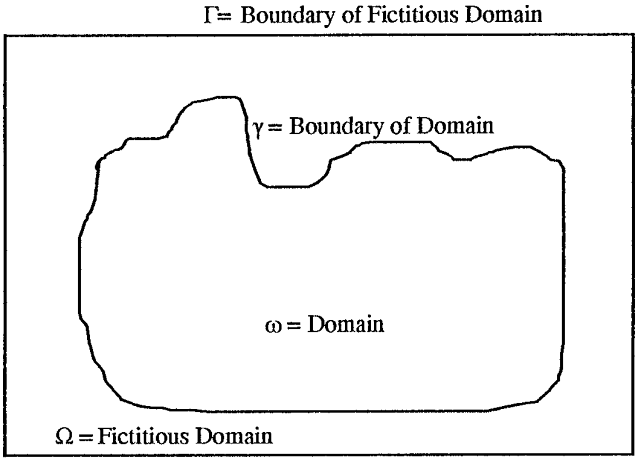

FIG. 1. Embedding of ω in Ω.

3. FICTITIOUS DOMAIN FORMULATIONS OF THE NEUMANN PROBLEM

3.1. *A Basic Fictitious Domain Formulation*

In order to solve the Neumann problem (2.1), (2.2) we embed ω in a larger domain Ω (see Fig. 1 for an illustration of such a situation), where we assume that ω is a $C^{0,1}$ domain, and $\overline{\omega} \subset \Omega$.

In the following parts of this article, we shall assume that Ω is a d-dimensional "box," that is, Ω is a product of intervals (as illustrated in Fig. 1 for $d = 2$). We consider then a closed subspace V of $H^1(\Omega)$ such that

$$\{v : v = \tilde{v}|_\omega, \tilde{v} \in V\} = H^1(\omega). \tag{3.8}$$

Typical choices for V are $H^1(\Omega)$, $H_0^1(\Omega)$, and the space $V_P(\Omega)$ defined by

$$V_P(\Omega) = \{v \in H^1(\Omega) : v \text{ is periodic on } \partial\Omega\}. \tag{3.9}$$

Suppose that $\Omega = (0, T)^d$ for some $L > 0$. Then the periodicity property in (3.9) means that $v(0, x_2, ..., x_d) = v(T, x_2, ..., x_d)$ for almost every $\{x_2, ..., x_d\} \in (0, T)^{d-1}$ with similar relations for the other $d - 1$ axis of coordinates directions. Next, we introduce a bilinear form $b : V \times V \to \mathbf{R}$ and a linear functional L: $V \to \mathbf{R}$, such that $b(\cdot, \cdot)$ is continuous and V-elliptic over $V \times V$, and L is continuous over V.

We can, for example, define b by

$$b(v, w) = \int_\Omega (b_0 v w + \mathbf{B}\nabla v \cdot \nabla w)\, dx \quad \forall v, w \in V, \tag{3.10}$$

where $b_0 \in L^\infty(\Omega)$, $b_0 \geq 0$, $b \neq 0$ and where

$$\begin{aligned} &\mathbf{B} \in L^\infty(\mathbf{R}^{d^2}), \quad \mathbf{B}(x)\xi \cdot \xi \\ &\quad \geq \beta|\xi|^2, \quad \text{a.e. on } \Omega\ \forall \xi \in \mathbf{R}^d, \end{aligned} \tag{3.11}$$

with β a positive constant. Actually, if $V = H_0^1(\Omega)$, we can take $b_0 = 0$; the properties of $\mathbf{B}$ imply that $b(\cdot, \cdot)$ is still strongly elliptic over $H_0^1(\Omega) \times H_0^1(\Omega)$.

Remark. The functions b_0 and $\mathbf{B}$ restricted to ω may coincide with a_0 and $\mathbf{A}$ but this is not a necessity; similarly, it is not necessary to have L related to f and g. Therefore $L = 0$ is a possible choice.

Next, we introduce the following subspaces of V:

$$\begin{aligned} H = \{v \in V : &\int_\omega (a_0 v \mu + \mathbf{A}\nabla v \cdot \nabla \mu)\, dx \\ &= \int_\omega f\mu\, dx + \langle g, \mu\rangle, \forall \mu \in V\} \end{aligned} \tag{3.12}$$

$$H_0 = \{v \in V : \int_\omega (a_0 v \mu + \mathbf{A}\nabla v \cdot \nabla \mu)\, dx = 0, \forall \mu \in V\}. \tag{3.13}$$

Assuming that the hypotheses on a_0, $\mathbf{A}$, f, g made in Section 2.2 hold, the Neumann problem (2.1), (2.2), or its variational formulation (2.7), has a unique solution; this fact combined with the inclusion hypothesis (3.8) implies that H is *nonempty*; in addition, we clearly have that H is a *closed convex* subset of V. Similar properties hold for H_0 which is therefore a nonempty closed subspace of V. We consider next the following problem:

$$\begin{aligned} &\tilde{u} \in H, \\ &b(\tilde{u}, v - \tilde{u}) \geq L(v - \tilde{u}) \quad \forall v \in H. \end{aligned} \tag{3.14}$$

Problem (3.14) is a classical variational inequality like those discussed in, e.g., [11, 7, 9]. It follows from the above references that the properties of $b(\cdot, \cdot)$, $L(\cdot)$, and H imply that problem (3.14) has a unique solution. Also, since $\tilde{u} + w \in H$, $\forall w \in H_0$, we obtain from (3.14) (taking $v = \tilde{u} + w$) that

$$b(\tilde{u}, w) \geq L(w) \quad \forall w \in H_0,$$

which implies in turn (since $-w$ also belongs to H_0) that

$$b(\tilde{u}, w) = L(w) \quad \forall w \in H_0.$$

We have thus shown that the solution of (3.14) is necessarily the solution of

$$\begin{aligned} &\tilde{u} \in H, \\ &b(\tilde{u}, v) = L(v) \quad \forall v \in H_0. \end{aligned} \tag{3.15}$$

The reciprocal property is obviously true since $b(\tilde{u}, v) = L(v)$, $\forall v \in H_0$ implies $b(\tilde{u}, v - \tilde{u}) = L(v - \tilde{u})$, $\forall v \in H$, which implies in turn

$$b(\tilde{u}, v - \tilde{u}) \geq L(v - \tilde{u}) \quad \forall v \in H.$$

It is also obvious that

$$\tilde{u}|_\omega = u, \tag{3.16}$$

where, in (3.16), u is the solution of problem (2.1), (2.2), (2.7).

3.2. *A Regularization and Fictitious Domain Method*

In this paragraph, we shall use the following notation:

$$a(v, w) = \int_\omega (\mathbf{A}\nabla v \cdot \nabla w + a_0 v w)\, dx \quad \forall v, w \in V, \tag{3.17}$$

$$l(v) = \int_\omega f v\, dx + \langle g, v\rangle \quad \forall v \in V. \tag{3.18}$$

We consider then the linear variational problem

$$\begin{aligned} &u_\varepsilon \in V,\\ &\varepsilon b(u_\varepsilon, v) + a(u_\varepsilon, v) = \varepsilon L(v) + l(v) \quad \forall v \in V, \end{aligned} \tag{3.19}$$

where, in (3.19), ε is a *positive* parameter. For the following convergence theorem we assume that $\mathbf{A}$ satisfies (2.4), $\mathbf{B}$ satisfies (3.11), that a and b are strongly elliptic bilinear functionals on V given by (3.17) and (3.10), L is a continuous linear functional on V, and l is given by (3.18) (hence also a continuous linear functional on V).

THEOREM 3.1. *Let ω be a $C^{0,1}$ domain, and let u, $\tilde{u}$, and u_ε be solutions of problems* (2.1), (2.2), (3.14), *and* (3.19), *respectively*; *then*

$$\begin{aligned} \lim_{\varepsilon\to 0} \|u_\varepsilon - \tilde{u}\|_{H^1(\Omega)} &= 0,\\ \lim_{\varepsilon\to 0} \varepsilon^{-1/2}\|u_\varepsilon - u\|_{H^1(\omega)} &= 0. \end{aligned} \tag{3.20}$$

Proof. In the following C will denote various constants.

(1) *Boundedness of* $\{u_\varepsilon\}_{\varepsilon>0}$. Let $\tilde{u}$ be the solution of problem (3.14). Taking $v = u_\varepsilon - \tilde{u}$ in (3.19) we obtain

$$\begin{aligned} &\varepsilon b(u_\varepsilon - \tilde{u}, u_\varepsilon - \tilde{u}) + a(u_\varepsilon - \tilde{u}, u_\varepsilon - \tilde{u})\\ &\quad = \varepsilon[L(u_\varepsilon - \tilde{u}) - b(\tilde{u}, u_\varepsilon - \tilde{u})]\\ &\qquad + l(u_\varepsilon - \tilde{u}) - a(\tilde{u}, u_\varepsilon - \tilde{u}). \end{aligned} \tag{3.21}$$

Since $\tilde{u}|_\omega = u$ (see (3.16)) it follows from (2.7), (3.12), (3.14), (3.17), and (3.18) that

$$a(\tilde{u}, v) = l(v) \quad \forall v \in V. \tag{3.22}$$

Taking $v = u_\varepsilon - \tilde{u}$ in (3.22) and combining with (3.21) we obtain

$$\begin{aligned} b(u_\varepsilon - \tilde{u}, u_\varepsilon - \tilde{u}) + \frac{1}{\varepsilon} a(u_\varepsilon - \tilde{u}, u_\varepsilon - \tilde{u}) &= L(u_\varepsilon - \tilde{u})\\ &\quad - b(\tilde{u}, u_\varepsilon - \tilde{u}). \end{aligned} \tag{3.23}$$

It follows from (3.23), from $\varepsilon > 0$, and from the ellipticity and continuity properties of a, b, L that

$$\beta'\|u_\varepsilon - \tilde{u}\|_V^2 \leq (\|L\| + \|b\|\,\|\tilde{u}\|_V)\|u_\varepsilon - \tilde{u}\|_V \quad \forall \varepsilon > 0, \tag{3.24}$$

where, in (3.24), $\beta' > 0$ and where $\|L\|$ and $\|b\|$ are defined by

$$\|L\| = \sup_v \frac{|L(v)|}{\|v\|_V}, \quad v \in V\backslash\{0\},$$

and

$$\|b\| = \sup_{v,w} \frac{|b(v, w)|}{\|v\|_V\|w\|_V}, \quad v \in V\backslash\{0\}, \quad w \in V\backslash\{0\}.$$

Relation (3.24) implies

$$\|u_\varepsilon - \tilde{u}\|_V \leq C \quad \forall \varepsilon > 0,$$

which implies in turn

$$\|u_\varepsilon\|_{H^1(\Omega)} \leq C \quad \forall \varepsilon > 0. \tag{3.25}$$

(2) *Weak convergence of* $\{u_\varepsilon\}_{\varepsilon>0}$: It follows from (3.25) and from the closedness of V in $H^1(\Omega)$ (which implies the weak closedness) that there exist $u^* \in V$ and a subsequence—still denoted by $\{u_\varepsilon\}_{\varepsilon>0}$—such that

$$\lim_{\varepsilon\to 0} u_\varepsilon = u^* \quad \text{weakly in } H^1(\Omega). \tag{3.26}$$

Combining (3.26) with (3.19) we obtain at the limit in (3.19) that

$$a(u^*, v) = l(v) \quad \forall v \in V;$$

i.e.,

$$u^* \in H. \tag{3.27}$$

Replacing v by $v - u_\varepsilon$ in (3.19) we obtain (taking into account the ellipticity of $a(\cdot, \cdot)$)

$$
\begin{aligned}
b(u_\varepsilon, v) &= L(v-u_\varepsilon) + b(u_\varepsilon, u_\varepsilon) \\
&\quad + \frac{1}{\varepsilon} a(u_\varepsilon, u_\varepsilon) + \frac{1}{\varepsilon}[l(v-u_\varepsilon) - a(v, v-u_\varepsilon)] \\
&\geq L(v-u_\varepsilon) + b(u_\varepsilon, u_\varepsilon) \\
&\quad + \frac{1}{\varepsilon}[l(v-u_\varepsilon) - a(v, v-u_\varepsilon)] \quad \forall v \in V.
\end{aligned} \tag{3.28}
$$

Suppose now that $v \in H$; we have then $v|_\omega = u$ which implies that

$$a(v, v - u_\varepsilon) = l(v - u_\varepsilon) \quad \forall v \in H,$$

which combined with (3.28) implies in turn that

$$b(u_\varepsilon, v) \geq L(v - u_\varepsilon) + b(u_\varepsilon)\, u_\varepsilon, \quad \forall v \in H. \tag{3.20}$$

Since $b(\cdot, \cdot)$ is positive definite over $V \times V$ we have, form (3.26),

$$\liminf_{\varepsilon \to 0} b(u_\varepsilon, u_\varepsilon) \geq b(u^*, u^*),$$

which combined with (3.29) implies

$$b(u^*, v) \geq L(v - u^*) + b(u^*, u^*) \quad \forall v \in H.$$

We have thus proved (taking (3.27) into account) that u^* is a solution of (3.14); since (3.14) has a unique solution we have $u^* = \tilde{u}$, which implies that the whole family $\{u_\varepsilon\}_{\varepsilon>0}$ converges to $\tilde{u}$.

(3) *Strong convergence of* $\{u_\varepsilon\}_{\varepsilon>0}$. Consider relation (3.23); we have just shown that u_ε converges weakly to $\tilde{u}$. Combining this result with (3.23) and taking into account the ellipticity properties of $a(\cdot, \cdot)$ and $b(\cdot, \cdot)$, we finally obtain the convergence properties (3.20). ▮

4. WAVELET AND FINITE ELEMENT-GALERKIN SOLUTION OF THE NEUMANN PROBLEM

4.1. *Numerical Approximations*

In this section we want to formulate a Galerkin solution of the regularized Neumann problem as posed in (2.7), where A and B are identity matrices and $a_0 = b_0 = \alpha > 0$.

Consider the space $V \subset H^1(\Omega)$ defined by (3.8) consisting of all elements of $H^1(\Omega)$ which are extensions of elements of $H^1(\omega)$ to Ω. We now consider any finite-dimensional subspace V_h of V (which could be defined by finite-elements, wavelets, or any other approximation scheme). We now consider the restriction of problem (2.7) to this finite-dimensional subspace. We have

Find u_h^ε in V_h such that

$$a(u_h^\varepsilon, v_h) + \varepsilon b(u_h^\varepsilon, v_h) = \varepsilon L(v_h) + l(v_h) \quad \forall v_h \in V_h. \tag{4.30}$$

Problem (4.30) has a unique solution in V_h.

4.2. *Error Estimates*

In this section, we assume that ω is a $C^{1,1}$ domain and $f \in L^2(\omega)$, $g \in H^{1/2}(\partial\omega)$. Then the solution u of problem (2.7) is in $H^2(\omega)$. In order to get error estimates for $\|u - u_h^\varepsilon\|_{H^1(\omega)}$ and $\|u - u_h^\varepsilon\|_{L^2(\omega)}$, where u_h^ε is the solution to (4.30), we need to extend the solution u of problem (2.7) from $H^2(\omega)$ into V. In [4], there is a basic extension result. We state it in the following theorem.

THEOREM 4.1. *Let ω be a bounded domain in $\mathbf{R}^d$ with a $C^{k,1}$ boundary for some integer $k \geq 0$ and $\omega \subset\subset \Omega$, where Ω is an open set. Then there is a bounded linear extension operator E from $H^{k+1}(\omega)$ into $H_0^{k+1}(\Omega)$ such that $Ev|_\omega = v$ and*

$$\|Ev\|_{H^{k+1}(\Omega)} \leq C(k, \omega, \Omega)\|u\|_{H^{k+1}(\omega)} \tag{4.31}$$

for all $v \in H^{k+1}(\omega)$.

Thus for the polygonal fictitious domain Ω, $\omega \subset\subset \Omega$, we can extend the solution u of the problem (2.7) from $H^2(\omega)$ to $H_0^2(\Omega)$, and especially for the square domain Ω, we can extend u from $H^2(\omega)$ to $H_P^2(\Omega)$, the space of periodic functions in $H^2(\Omega)$. Let the extension u be denoted by Eu. We have the following result [5].

LEMMA 4.2. *Assume that ω is a bounded domain in $\mathbf{R}^d$ with a $C^{1,1}$ boundary and $\omega \subset\subset \Omega$, where Ω is a polygonal domain. Then there exists a constant C_1 such that*

$$
\begin{aligned}
\|u_h^\varepsilon - u\|_{H^1(\omega)} \leq C_1 \inf_{v_h \in V_h} \{&\|Eu - u_h^\varepsilon\|^2_{H^1(\Omega)} + \varepsilon\|\tilde{f}\|^2_{L^2(\Omega)} \\
&+ \varepsilon\|Eu\|^2_{H^1(\Omega)}\}^{1/2},
\end{aligned} \tag{4.32}
$$

where u is the solution of problem (2.7) *and u_h^ε is the solution of problem* (4.30).

4.3. *Finite Element Discretization*

In this section we specialize the results in (4.1) and (4.2) to the case of finite elements. Let us first give a brief description of the finite element spaces used to obtain the error estimates in the following paragraphs. Let $\mathcal{T}_h$ be a regular triangulation of the polygonal domain Ω. We would like to use finite elements, d-simplices of type (k), for integer $k > 0$ (other finite elements can be used). The finite element spaces V_h associated with the finite elements d-simplices of type (k) are given by

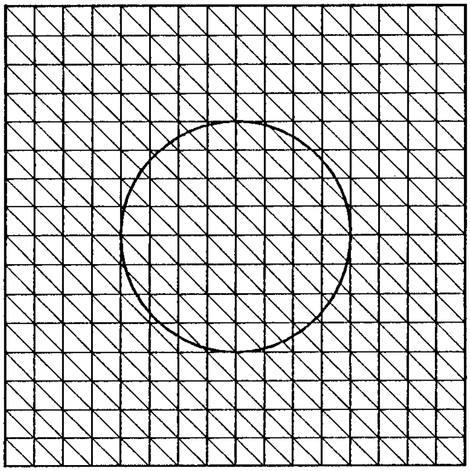

FIG. 2. Finite element grid with mesh size $h = \frac{1}{8}$.

$$V_h := \{v_h : v_h \in H_0^1(\Omega) \cap \mathbf{C}^0(\overline{\Omega}), v_h|_T \in P_k, \forall T \in \mathcal{T}_h\}, \tag{4.33}$$

where P_k is the space of the polynomials in n variables of degree $\leq k$.

Let $\{\Psi_i\}_{i=1}^N$ be the standard basis of the finite element space V_h, where N is the dimension of V_h and $\{d_i\}_{i=1}^N$ is the set of the mesh nodes; it satisfies the relation

$$\psi_i(d_j) = \delta_{ij} = \begin{cases} 1, & i = j, \\ 0, & i \neq j, \end{cases}$$

for $1 \leq i, j \leq N$. Also for any v_h in V_h, we have

$$v_h = \sum_{i=1}^N v_h(d_i)\psi_i.$$

The V_h-interpolant is defined by

$$\Pi_h v = \sum_{i=1}^N v(d_i)\psi_i,$$

for any $v \in C^0(\overline{\Omega})$. There are estimates of the interpolation error in [2]. We will use the following.

THEOREM 4.3. *If $k > d/2 - 1$, then there exists a constant C_2 independent of h such that, for any function $v \in H^{k+1}(\Omega) \cap H_0^1(\Omega)$,*

$$\|v - \Pi_h v\|_{H^1(\Omega)} \leq C_2 h^k \|v\|_{H^{k+1}(\Omega)}. \tag{4.34}$$

Let us assume that the solution u of problem (2.7) verifies $u \in H^{k+1}(\omega)$ for an integer $k > \max\{0, d/2 - 1\}$. Suppose also that ω is a bounded domain with a $C^{k,1}$ boundary, strictly contained in the polygonal open set Ω. We obtain the following H^1 error estimate [5].

THEOREM 4.4. *Let ω be a bounded C^{k+1} domain in $\mathbf{R}^d$, where k is an integer satisfying $>\max\{0, d/2 - 1\}$ and where $\overline{\omega} \subset \Omega$, which is a bounded polygonal open set. If the solution u of problem (2.7) verifies $u \in H^{k+1}(\omega)$, then there exists a constant C_3 independent of h such that*

$$\|u_h^\varepsilon - u\|_{H^1(\omega)} \leq C_3\{h^k\|u\|_{H^{k+1}(\omega)} + \sqrt{\varepsilon}\|\tilde{f}\|_{L^2(\Omega)} + \sqrt{\varepsilon}\|u\|_{H^{k+1}(\omega)}\}, \tag{4.35}$$

where u_h^ε is the solution of problem (4.30) for V_h as in (4.33) and $\varepsilon > 0$.

Therefore the optimal choice of ε is $\varepsilon = Mh^{2s}$, where M is constant and $s \geq k$ so that $\|u - u_h^\varepsilon\|_{H^1(\omega)}$ is of order h^k.

For the L^2 error estimate, we consider the following auxiliary problem:

TABLE I

$\|u - u_h^\varepsilon\|_{H^1(\omega)}/\|u\|_{H^1(\omega)}$ for $u(x, y) = x^3 - y^3$ for the Finite Element Method

ε	$h = \frac{1}{8}$	$h = \frac{1}{16}$	$h = \frac{1}{32}$
10^{-1}	1.27759362699	1.62154953409	2.16374221811
10^{-2}	0.32358749061	0.26197911257	0.29164753716
10^{-3}	0.19417803703	$8.3662335694 \times 10^{-2}$	$5.0478305305 \times 10^{-2}$
10^{-4}	0.18043329784	$6.5094253508 \times 10^{-2}$	$2.5674105973 \times 10^{-2}$
10^{-5}	0.17899468270	$6.3208218876 \times 10^{-2}$	$2.3200437070 \times 10^{-2}$
10^{-6}	0.17884885920	$6.3018799334 \times 10^{-2}$	$2.2953287236 \times 10^{-2}$
10^{-7}	0.17883425279	$6.2999847513 \times 10^{-2}$	$2.2928574657 \times 10^{-2}$
10^{-8}	0.17883279190	$6.2997952230 \times 10^{-2}$	$2.2926103423 \times 10^{-2}$
10^{-9}	0.17883264581	$6.2997762701 \times 10^{-2}$	$2.2925856300 \times 10^{-2}$
10^{-10}	0.17883263120	$6.2997743748 \times 10^{-2}$	$2.2925831587 \times 10^{-2}$

TABLE II

$\|u - u_h^\varepsilon\|_{L^2(\omega)}/\|u\|_{L^2(\omega)}$ for $u(x, y) = x^3 - y^3$ for the Finite-Element Method

ε	$h = \frac{1}{8}$	$h = \frac{1}{16}$	$h = \frac{1}{32}$
10^{-1}	1.48056340340	1.32677581622	1.23291488149
10^{-2}	0.37017875130	0.21327731659	0.16603820621
10^{-3}	0.21946578156	$6.6884846802 \times 10^{-2}$	$2.8487414845 \times 10^{-2}$
10^{-4}	0.20345479970	$5.1556945153 \times 10^{-2}$	$1.4246838113 \times 10^{-2}$
10^{-5}	0.20178058788	$4.9997028789 \times 10^{-2}$	$1.2813815642 \times 10^{-2}$
10^{-6}	0.20161092886	$4.9840331005 \times 10^{-2}$	$1.2670335191 \times 10^{-2}$
10^{-7}	0.20159393549	$4.9824652763 \times 10^{-2}$	$1.2655985068 \times 10^{-2}$
10^{-8}	0.20159223587	$4.9823084852 \times 10^{-2}$	$1.2654550035 \times 10^{-2}$
10^{-9}	0.20159206590	$4.9822928061 \times 10^{-2}$	$1.2654406531 \times 10^{-2}$
10^{-10}	0.20159204898	$4.9822912381 \times 10^{-2}$	$1.2654392181 \times 10^{-2}$

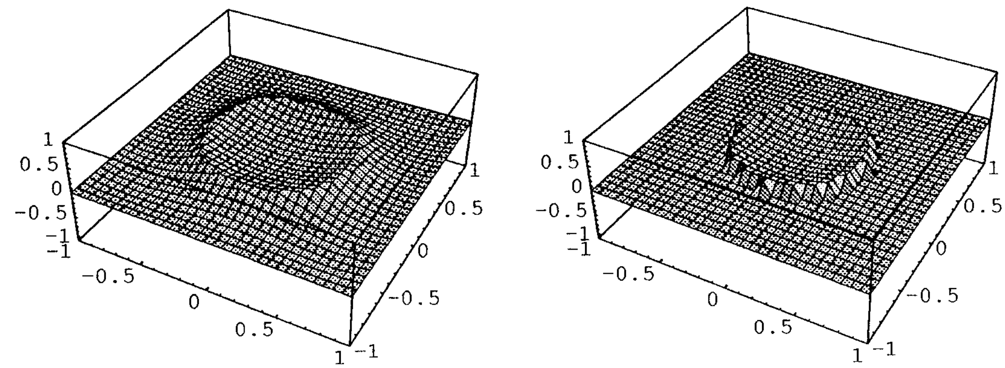

FIG. 3. The left figure is the graph of u_h^ε and the right one is the graph of $u_h^\varepsilon X_\omega$, where X_ω is the characteristic function of ω for $\varepsilon = 10^{-6}$.

Find ϕ in $H^1(\omega)$ such that

$$\int_\omega (\alpha\phi v + \nabla\phi \cdot \nabla v)\, dx = \int_\omega (u - u_h^\varepsilon) v\, dx \quad \forall v \in H^1(\omega). \tag{4.36}$$

Since $u - u_h^\varepsilon \in H^1(\omega)$, we have

$$\|\phi\|_{H^2(\omega)} \leq C_5 \|u - u_h^\varepsilon\|_{L^2(\omega)}. \tag{4.37}$$

Also we consider the auxiliary problem utilizing the fictitious domain penalty approach,

Find ϕ^ρ in $H_0^1(\Omega)$ such that

$$a(\phi^\rho, v) + \rho b(\phi^\rho, v) = \int_\omega (u - u_h^\varepsilon) v\, dx \quad \forall v \in H_0^1(\Omega). \tag{4.38}$$

and the finite element approximation of problem (4.38)

Find ψ_h^ρ in V_h such that

$$a(\psi_h^\rho, v_h) + \rho b(\psi_h^\rho, v_h) = \int_\omega (u - u_h^\varepsilon) v_h\, dx \quad \forall v_h \in V_h. \tag{4.39}$$

Problems (4.38) and (4.39) have a unique solution in $H_0^1(\Omega)$ and V_h, respectively.

The L^2 error estimate is obtained from the following result [5].

THEOREM 4.5. *Assume that the conditions in Theorem* 4.4 *hold and $d \leq 3$. Then there exists a constant C_4 independent of h such that*

$$\begin{aligned} \|u - u_h^\varepsilon\|_{L^2(\omega)} \leq C_4 \{ &(h + \sqrt{\rho})((h^k + \sqrt{\varepsilon})\|u\|_{H^{k+1}(\omega)} \\ &+ \sqrt{\varepsilon}\|\tilde{f}\|_{L^2(\Omega)}) + \varepsilon \left(\frac{h}{\sqrt{\rho}} + 1\right) \\ &\left\{\left(\frac{h^k}{\sqrt{\varepsilon}} + 1\right)\|u\|_{H^{k+1}(\omega)} + 2\|\tilde{f}\|_{L^2(\Omega)}\right\}\}, \end{aligned} \tag{4.40}$$

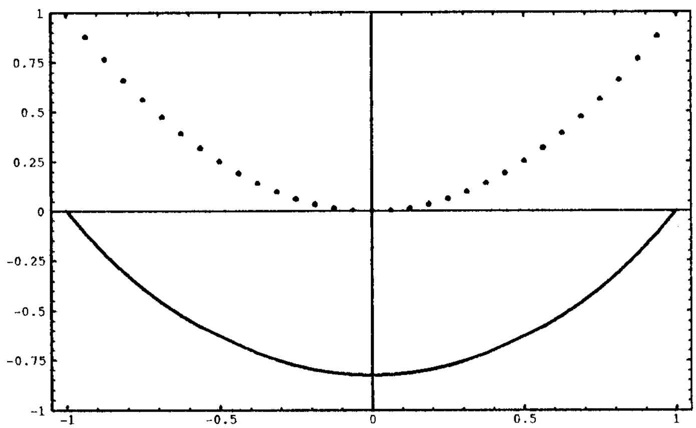

FIG. 4. The variations of $x \to u_h^\varepsilon(x, 0)$ (in solid line) and $x \to u(x, 0)$ (in dotted line), where $u(x, y) = x^2 + y^2$ for $\varepsilon = 1.0$.

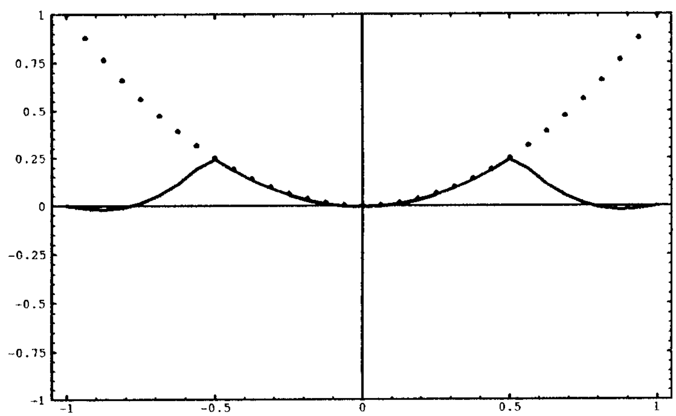

FIG. 5. The variations of $x \to u_h^\varepsilon(x, 0)$ (in solid line) and $x \to u(x, 0)$ (dotted line), where $u(x, y) = x^2 + y^2$ for $\varepsilon = 10^{-3}$.

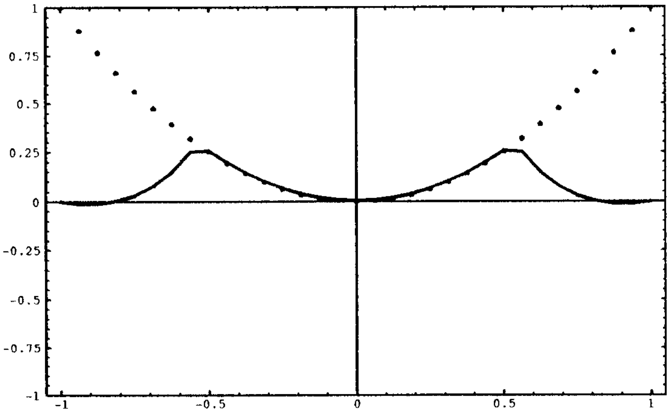

FIG. 6. The variations of $x \to u_h^\varepsilon(x, 0)$ (solid line) and $x \to u(x, 0)$ (dotted line), where $u(x, y) = x^2 + y^2$ for $\varepsilon = 10^{-6}$.

where u is the solution of problem (2.7), u_h^ε *is the solution of problem* (4.30), *and* ε, $\rho > 0$.

Let $\varepsilon = M_1 h^{2s}$ and $\rho = M_2 h^{2l}$, where M_1, M_2 are constants and s, l are integers. Then the optimal choices of ε and ρ are $s \geq k$ and $s \geq l > 0$ so that $\|u - u_h^\varepsilon\|_{L^2(\omega)}$ is of order h^{k+1}.

4.4. *Wavelet Discretization*

Let ϕ be the Daubechies scaling function of order N ($N \geq 3$) [3]. Define $\phi_{j,k} := 2^{j/2}\phi(2^j x - k)$ for $k, j \in \mathbf{Z}$. We assume $\Omega = (-s, s) \times (-s, s)$, where s is a positive integer. Set

$$V_j := \Big\{ v \in L^2(\Omega) : v(x, y) = \sum_{k,l \in \mathbf{Z}} c_{k,l}\phi_{j,k}(x)\phi_{j,l}(y), x \in \Omega, c_{k,l} = c_{k+2^j 2s, l+2^j 2s} \Big\}.$$

V_j (resp. u_j) corresponds to V_h (resp. u_h) described in Section 4.1 with $h = 1/2^j$. Under the assumptions of Theorems 4.4 and 4.5, the analysis of [15, 8] gives

$$\|u - u_j^\varepsilon\|_{H^1(\omega)} = O(2^{-\min(N,k)j} + \sqrt{\varepsilon})$$

and

$$\|u - u_j^\varepsilon\|_{L^2(\omega)} = O(2^{-2\min(N,k)j} + \sqrt{\varepsilon}).$$

5. NUMERICAL EXPERIMENTS

5.1. *Finite Element Method*

We consider the following test problems. Let $\omega = \{(x, y) : x^2 + y^2 < \frac{1}{16}\}$, let $\Omega = (-1, 1) \times (-1, 1)$, and let $u(x, y) = x^2 + y^2$ (resp. $u(x, y) = x^3 - y^3$) be the solution of the Neumann problem

$$u - \Delta u = f \quad \text{in } \omega,$$
$$\frac{\partial u}{\partial n} = g \quad \text{on } \gamma;$$

we then have $f(x, y) = x^2 + y^2 - 4$ and $g(x, y) = \frac{1}{2}$ (resp. $f(x, y) = x^3 - y^3 - 6(x - y)$ and $g(x, y) = 12(x^3 - y^3)$).

In numerical experiments, we use 2-simplices of type (1) finite elements, so

$$V_h = \{v_h : v_h \in H_0^1(\Omega) \cap \mathbf{C}^0(\overline{\Omega}), v_h|_T \in P_1, \forall T \in \mathcal{T}_h\},$$

where $\mathcal{T}_h$ is the regular uniform triangulations of Ω (e.g., see Fig. 2) and P_1 is the space of the polynomials in two variables of degree 1.

The $\tilde{f}$ in (4.30) is given by $\tilde{f} = f$ in Ω. The line integral along $\partial\omega$ in (4.30) is evaluated by Simpson's composite rule. The mesh sizes are $\frac{1}{8}$, $\frac{1}{16}$, and $\frac{1}{32}$. For the finite element $T \in \mathcal{T}_h$ with area $(T \cap \omega) \neq 0$ and area$(T \cap \omega) \neq$ area(T),

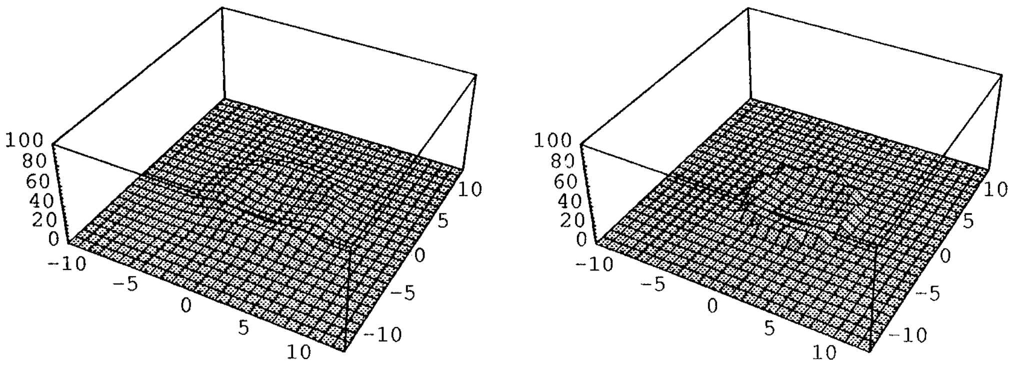

FIG. 7. The wavelet Galerkin solution for $\varepsilon = 1$.

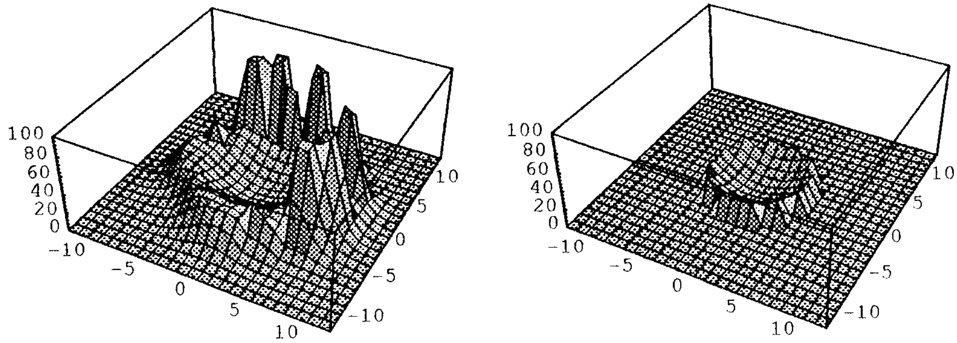

FIG. 8. The wavelet Galerkin solution for $\varepsilon = 10^{-3}$.

the area $(T \cap \omega)$ has to be computed accurately enough to obtain good results. The linear systems obtained from problem (4.30) have been solved via a *Cholesky factorization*. The CPU times for solving problem (4.30) with a given ε on a Sparcstation 2 are 1.8 s, 7.6 s, and 193.4 s for mesh sizes $\frac{1}{8}$, $\frac{1}{16}$, and $\frac{3}{12}$, respectively.

For the test problem with $u(x, y) = x^3 - y^3$, we list the relative H^1 and L^2 errors with ε going from 10^{-1} to 10^{-10} in Tables I and II. The H^1 errors are of order h, the L^2 errors being of order h^2 if ε is small enough. These are what we expect from Theorems 4.4 and 4.5. For the other test problem with $u(x, y) = x^2 + y^2$, the errors are too good to obtain the orders of errors similar to those of $u(x, y) = x^3 - y^3$.

For the test problem with $u(x, y) = x^2 + y^2$, the surface graphs of the approximate solutions with $h = \frac{1}{16}$ are shown in Fig. 3 for $\varepsilon = 10^{-6}$. In Fig. 3, the left figure is the graph of u_h^ε and the right one is the graph of $u_h^\varepsilon X_\omega$, where X_ω is the characteristic function of ω. Also in Figs. 4, 5, and 6 the variations of $x \to u_h^\varepsilon(x, 0)$ (solid line) and $x \to u(x, 0)$ (dotted line) are shown for $\varepsilon = 1$, 10^{-3}, and 10^{-6}. If $\varepsilon = 1.0$, it is not surprising that the approximate solution is really far away from the exact solution in ω. As ε becomes smaller, the approximate solution is quite accurate on ω. Even near the boundary $\partial\omega$, the approximate solution is quite accurate.

5.2. *Wavelet–Galerkin Method*

Let us approximate u^ε by $u_L^\varepsilon \in V_L, j \in \mathbf{Z}^+$, as in Section 4.4. Also we sample the characteristic function χ_ω, the functions f and extended g in V_l (l and L can be distinct). Then, by precomputing the connection coefficients

$$\Gamma_{m,n} := \int \phi(x)\phi_m'(x)\phi_n'(x)\,dx,$$

one can derive the desired linear system for the unknowns.

Remark. (1) It is convenient to choose the expansion spaces for u_L^ε and χ_ω to be the same as those used to calculate

$$\int_\omega (\nabla u \nabla v + uv)\,dx.$$

(2) To calculate the boundary integral on the right-hand side, we use the uniform geometric measure approach introduced in [14] to avoid numerical integration, since the

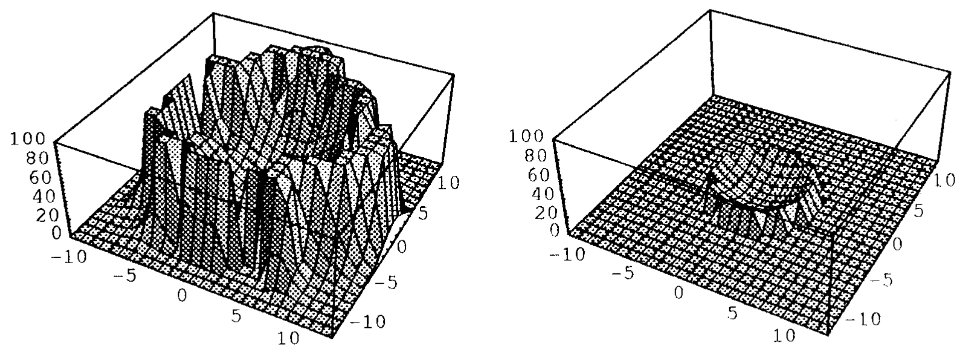

FIG. 9. The wavelet Galerkin solution for $\varepsilon = 10^{-6}$.

TABLE III

Comparative Times on a SparcStation Using Matlab Coding

Time consumed	Min
$L = 0$:	15
$L = 1$:	168

latter requires the knowledge of the parametrization of $\partial\omega$. Briefly speaking, one can write

$$\int_{\partial\omega} g\, ds = \int_{\mathbf{R}^2} g\, d\mu,$$

where μ is a Radon measure supported on $\partial\omega$. In fact,

$$\mu = \nabla_{\chi_\omega} \cdot \frac{\nabla F}{|\nabla F|} \tag{5.41}$$

if $\partial\omega$ is given by $\partial\omega = \{(x, y) : F(x, y) = 0\}$ for some Lipschitz function F. Therefore, if we sample g, χ_ω, F in V_l as g_l, $\chi_{\omega,l}$, F_l, and approximately μ by μ_l, which is calculated accordingly by the formula (5.41), one can show that

$$\int_{\mathbf{R}^2} g_l\, d\mu_l \to \int_{\partial\omega} g\, d\mu$$

as $l \to +\infty$; see [14] for the proof. Here we choose $l \gg L$ for better accuracy.

EXAMPLE 5.1. Let

$$\omega = \{x^2 + y^2 \le 5^2\}$$
$$\Omega = \{|x|, |y| \le 15\}$$
$$\Lambda = \{(i, j) : i, j = -15 \times 2^L, \ldots, 15 \times 2^L - 5\},$$

and we want to solve

$$\Delta u + u = f, \quad \frac{\partial u}{\partial n} = g \quad \text{on } \partial\omega.$$

Here we assume that we use the order 3 translated Daubechies scaling functions as our basis. The test problem is chosen so that $u = x^2 + y^2$ is the desired solution. We solve for the numerical solution at level $L = 0, 1$. Once the linear system is set, we use LU decomposition to solve it. In Figs. 7, 8, and 9 we see graphs of solutions of the solution to this test problem for variable values of the regularizing parameter ε. In Table III we see a comparison of the time consumed for different levels, and in the following section we see a comparison with the finite element computations given in the previous section. In this paper we are more concerned with checking the accuracy of these methods. In later papers we will go to methods which will dramatically speed up these calculations yielding the same accuracy (such as multigrid and parallel computation; see [6, 12]).

In Tables IV, V we present the relative errors $E_\omega^{\varepsilon,L}$ with respect to different choices of ε and the levels $L = 0, 1$,

TABLE IV

Relative Error in H^1 Norm; $\|u^{\varepsilon,L} - u\|_{H^1(\omega)}/\|u\|_{H^1(\omega)}$ for $u(x, y) = x^2 - y^2$ for the Wavelet Method

ε	$L = 0$	$L = 1$
10^0	0.72312811620280	0.70420788736429
10^{-1}	0.24079518419690	0.20971773207275
10^{-2}	0.69763698457707	0.13364955388352
10^{-3}	0.71127229550499	0.02133194677591
10^{-4}	0.02153308376562	0.13696729249436
10^{-5}	0.02418248442799	0.00968907358125
10^{-6}	0.02697287795870	0.00923777387524
10^{-10}	0.02491507164637	0.00934298716397

TABLE V

Relative Error in L^2 Norm; $\|u^{\varepsilon,L} - u\|_{L^2(\omega)}/\|u\|_{L^2(\omega)}$ for $u(x, y) = x^2 + y^2$ for the Wavelet Method

ε	$L = 0$	$L = 1$
1	0.64011168983714	0.60030587469127
10^{-1}	0.18728365752675	0.14122301303582
10^{-2}	0.06349181648207	0.02920589711123
10^{-3}	0.06433735001700	0.00359286263457
10^{-4}	0.00563482997730	0.00196723305079
10^{-5}	0.00280148379091	$4.461257406785745 \times 10^{-4}$
10^{-6}	0.00201636549800	$5.006539897281224 \times 10^{-4}$
10^{-10}	0.00192268309090	$5.194671480165910 \times 10^{-4}$

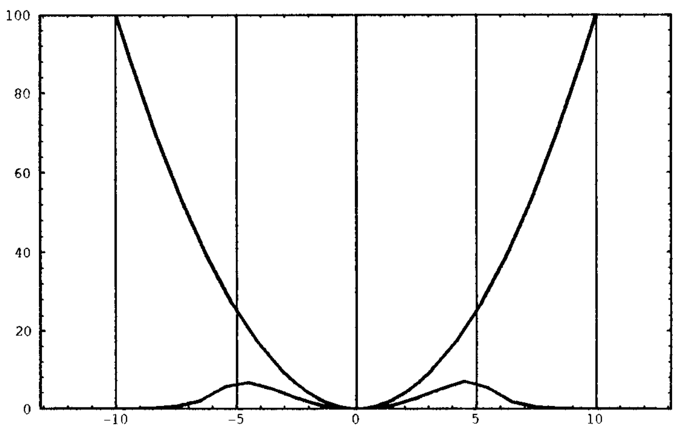

FIG. 10. Solution u_ε, for $\varepsilon = 1$, restricted to $y = 0$.

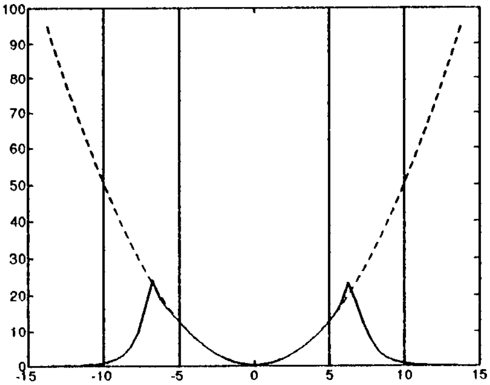

FIG. 11. Solution u^{ε}, for $\varepsilon = 10^{-4}$, restricted to $y = 0$.

TABLE VI

Comparison of Relative L^2 Error Obtained by Wavelet Method and Finite Element Method

ε	Wavelet	Finite element
10^{-1}	0.19653	1.38506
10^{-2}	0.06411	0.34298
10^{-3}	0.32074	0.09031
10^{-4}	0.01717	0.14601
10^{-5}	0.05829	0.15172
10^{-6}	0.02049	0.15229
10^{-7}	0.01350	0.15235
10^{-8}	0.01349	0.15235
10^{-9}	0.01359	0.15236
10^{-10}	0.01359	0.15236

in H^1 and L^2 norm. More specifically, if we denote the wavelet solution by $u^{\varepsilon,L}$, then

$$E_{\omega}^{\varepsilon,L} := \frac{\|u^{\varepsilon,L} - u\|_{L^2(\omega)}}{\|u\|_{L^2(\omega)}},$$

or

$$E_{\omega}^{\varepsilon,L} := \frac{\|u^{\varepsilon,L} - u\|_{H^1(\omega)}}{\|u\|_{H^1(\omega)}}.$$

These can be calculated numerically as follows.

Assume we have the expansions of $u^{\varepsilon,L}$ and u^L at the level L. Also we suppose that χ_{ω}^L is the expansion of the characteristic function χ_{ω} of ω at level L. Then

$$\|u^{\varepsilon,L} - u\|_{L^2(\omega)} = \|(u^{\varepsilon,L} - u)\chi_{\omega}^L\|_{L^2(\omega)}.$$

Similarly, using connection coefficients for the first-order derivative, one can calculate the expansions of

$$\frac{\partial(u^{\varepsilon,L} - u^L)}{\partial x}, \frac{\partial(u^{\varepsilon,L} - u^L)}{\partial u}$$

and

$$\frac{\partial u^L}{\partial x}, \frac{\partial u^L}{\partial y}.$$

Then

$$\left\|\frac{\partial}{\partial x}(u^{\varepsilon,L} - u^L)\right\|_{L^2(\omega)} = \left\|\frac{\partial(u^{\varepsilon,L} - u^L)}{\partial x}\chi_{\omega}^L\right\|_{L^2(\omega)},$$

etc.

In Figs. 10, 11, and 12, we see comparisons of these same solutions for slices near the middle of the fictitious domain Ω with respect to different ε's.

5.3. *Comparison of Finite Element and Wavelet Accuracy*

In Table VI the comparison between the numerical results obtained by the wavelet method and those obtained by the finite element method is presented with ε varying from 10^{-1} to 10^{-10}. Both methods have been applied to the same test problem,

$$u - \Delta u = x^2 + y^2 - 4 \quad \text{in } \omega,$$
$$\frac{\partial u}{\partial n} = g \quad \text{on } \gamma,$$

whose exact solution is $u(x, y) = x^2 + y^2$. For both methods, the geometry of the fictitious domain is the same; the mesh is the uniform mesh and the number of mesh points in the x-direction and the y-direction is 33. But the basis for the wavelet method are order 3 scaling functions and the finite dimensional subspace for the finite element

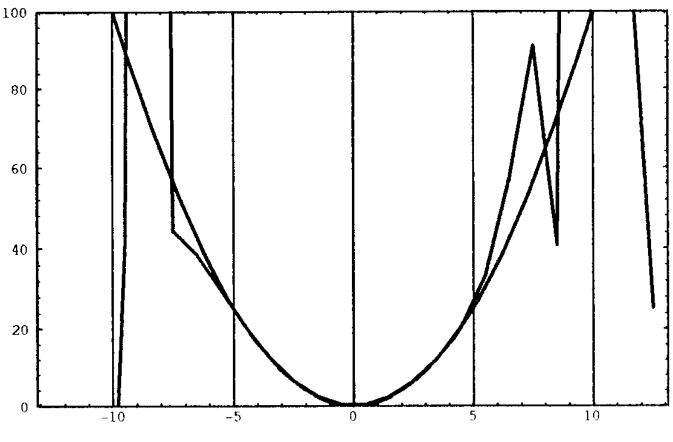

FIG. 12. Solution u^{ε}, for $\varepsilon = 10^{-6}$, restricted to $y = 0$.

method is the one defined in 5.2 which consists of piecewise continuous linear functions.

The better behavior of the relative L^2-error obtained by wavelet approximation is expected. In [10] it is pointed out that the approximation of the first-order differential operator associated with the genus-3 Daubechies wavelet basis is the 9-point finite difference operator with truncation error of order 4. By Theorem 4.5, the finite element approximation with piecewise continuous linear functions is of second order.

Also in the wavelet approximation, the part $\int_\omega (vw + \nabla v \cdot \nabla w)\, dx\, dy$ and the boundary integral are calculated systematically using the characteristic function χ_ω and its corresponding measure $-\nabla \chi_\omega \cdot \mathbf{n}$. A parametrization of the boundary curve was not required or used. Also in the computation of the $\int_\omega (vw + \nabla v \cdot \nabla w)\, dx\, dy$ in the finite element approximation, we need to do it *accurately* over these elements T with area$(T \cap \omega) \neq 0$ and area$(T \cap \omega) \neq$ area(T) in the triangulation of the fictitious domain Ω to obtain good results.

The numerical solutions of the finite element method have no oscillations over the fictitious domain and approximate the solutions very well near the boundary of ω for small ε (see Fig. 3, for instance). On the other hand, the numerical solution of the wavelet method has significant oscillation outside the actual domain ω (see Figs. 8, 9, and 12), which may be because of the approximation of the boundary integral.

6. CONCLUSION

In this paper we have seen that the wavelet–Galerkin method is comparable to the classical finite element problem and has inherently more accuracy if linear finite elements are used. It is a simple matter to change the wavelet code to implement Daubechies coefficients of higher rank to get more accurate solutions, and of course, at a cost of slower running time. The principal difference between the two methods in this paper was in the coding for the integration around the boundary of the given domain ω. For the finite element method it was necessary to use an explicit parametrization of the boundary (in this case as a circle), and for the wavelet method the calculation of the boundary integral resulted from differentiating the characteristic function of the domain. For some problems in higher dimensions the parametrization of the boundary would be more difficult and having a code that computes such integrals automatically will be beneficial, although there is some cost in the implementation, but no cost in the coding time. One consequence of the work in this paper is that one sees that the fictitious domain method here works for the boundary of an essentially arbitrary bounded domain (with the assumption that the boundary is rectifiable), and as remarked above, there is a difference in the coding of the boundary integrals for both methods (requiring a knowledge of the parametrization of the boundary curve for the finite element method).

In future papers we will explore the extension of these ideas to the multigrid and parallal processing arena. The ultimate goal is to find a general solution method which involves multilevel localized analysis, doing calculations at different scales (or several scales at the same time a la multigrid) at different regions of the domain considered, depending on the nature of how much computational power one needs from one point to another.

REFERENCES

1. P. G. Ciarlet, "Basic Error Estimates for Elliptic Problems, *Handbook of Numerical Analysis, Vol. II,* edited by P. G. Ciarlet and J. L. Lions (North-Holland, Amsterdam, 1991).
2. P. G. Ciarlet, *The Finite Element Methods for Elliptic Problems* (North-Holland, Amsterdam, 1987).
3. I. Daubechies, *Comm. Pure Appl. Math.* **41,** 906 (1988).
4. D. Gilbarg and N. S. Trudinger, *Elliptic Partial Differential Equations of Second Order* (Springer-Verlag, Berlin, 1983).
5. R. Glowinski and T. W. Pan, *Calcolo* **29,** 125 (1992).
6. R. Glowinski, A. Rieder, R. O. Wells, and X. Zhou, Computational Mathematics Laboratory TR93-06, Rice University, 1993 *Model. Math. Anal. Numer.* (1996, to appear).
7. R. Glowsinki, *Numerical Methods for Nonlinear Variational Problems,* Series in Computational Physics (Springer-Verlag, New York, 1984).
8. R. A. Gopinath, W. M. Lawton, and C. S. Burrus, in *Proceedings, ICASSP-91. IEEE, 1991.*
9. N. Kikuchi and J. T. Oden, *Contact Problems in Elasticity: A Study of Variational Inequalities and Contact Problems* (SIAM, Philadelphia, 1988).
10. K. McCormick and R. O. Wells, *Math. Comput.,* **63** (207), 155 (1994).
11. J. L. Lions, R. Glowinski, and R. Tremolieres, *Numerical Analysis of Variational Inequalities.* (North-Holland, Amsterdam, 1981).
12. A. Rieder, R. O. Wells Jr., and X. Zhou, *Appl. Comput. Harmonic Anal.* **1,** 355 (1994).
13. G. Strang and G. J. Fix, *An Analysis of the Finite Element Method* (Prentice-Hall, Englewood Cliffs, NJ, 1973).
14. R. O. Wells and X. Zhou, Technical Report 92-02, Computational Mathematics Laboratory, Rice University, 1992 Numer. *Math.* **70,** 379 (1995).
15. R. O. Wells and X. Zhou, "Wavelet Interpolation and Approximate Solutions of Elliptic Partial Differential Equations," in *Noncompact Lie Groups,* edited by R. Wilson and E. A. Tanner (Kluwer, Dordrecht, 1994); in *Proceedings, NATO Advanced Research Workshop,* to appear.